

Waveplate analyzer using binary magneto-optic rotators

Xiaojun Chen¹, Lianshan Yan¹, and X. Steve Yao^{1,2}

¹. General Photonics Corp. Chino, CA, 91710, USA Tel: 909-590-5473 Fax: 909-902-5535

². Polarization Research Center and Key Laboratory of Opto-electronics Information and Technical Science (Ministry of Education), Tianjin University, Tianjin 300072, China

*Corresponding Author: syao@generalphotonics.com

Abstract: We demonstrate a simple waveplate analyzer to characterize linear retarders using magneto-optic (MO) polarization rotators. The all-solid state device can provide highly accurate measurements for both the retardation of the waveplate and the orientation of optical axes simultaneously.

©2007 Optical Society of America

OCIS codes: (120.5410) Polarimetry; (080.2730) Geometrical optics, matrix methods; (060.2300) Fiber measurements; (260.5430) Polarization

References and links

1. D. Goldstein, "Polarized light," (Second Edition, Marcel Dekker, Inc., NY, 2003).
2. E. Collett, *Polarized light: Fundamentals and Applications*, (Marcel Dekker, New York, 1993) pp. 100-103.
3. H. G. Jerrard, "Optical compensators for measurement of elliptical polarization," *J. Opt. Soc. Am.* **38**, 35-59 (1948).
4. D. H. Goldstein, "Mueller matrix dual-rotating retarder polarimeter," *Appl. Opt.* **31**, 6676-6683 (1992).
5. E. Dijkstra, H. Meekes, and M. Kremers, "The high-accuracy universal polarimeter," *J. Phys. D* **24**, 1861-1868 (1991).
6. P. A. Williams, A. H. Rose, and C. M. Wang, "Rotating-polarizer polarimeter for accurate retardance measurement," *Appl. Opt.* **36**, 6466-6472 (1997).
7. D. B. Chenault and R. A. Chipman, "Measurements of linear diattenuation and linear retardance spectra with a rotating sample spectropolarimeter," *Appl. Opt.* **32**, 3513-3519 (1993).
8. L. Shyu, C. Chen, and D. Su, "Method for measuring the retardation of a wave plate," *Appl. Opt.* **32**, 4242-4250 (1993).
9. J. E. Hayden and S. D. Jacobs, "Automated spatially scanning ellipsometer for retardation measurements of transparent materials," *Appl. Opt.* **32**, 6256-6263 (1993).
10. H. Takasaki, M. Isobe, T. Masaki, A. Konda, I. Agatsuma, and Y. Watanabe, *Appl. Opt.* **3**, 343-350 (1964).
11. H. F. Hazebroek and A. A. Holscher, *J Phys. E* **6**, 822-826 (1973).
12. T. Oakberg, "Measurement of waveplate retardation using a photoelastic modulator," *Proc. SPIE* **3121**, 19-22, (1997).
13. K. B. Rochford and C. M. Wang, "Accurate interferometric retardance measurements," *Appl. Opt.* **36**, 6473-6479 (1997).
14. X. S. Yao, L. S. Yan, and Y. Shi, "Highly repeatable all-solid-state polarization-state generator," *Opt. Lett.* **30**, 1324-1327 (2005)
15. X. S. Yao, X. Chen, and L.S. Yan, "Self-calibrating binary polarization analyzer" *Opt. Lett.* **31**, 1948-1950 (2006)
16. M. Born and E. Wolf, *Principle of optics: Electromagnetic theory of propagation, interference and diffraction of light*, (7th Edition, University Press, Cambridge, UK, 1999).

1. Introduction

Optical waveplates for generating linear retardations are one of the most important components for polarization-related analysis and control [1]. Accurate measurement of retardation and optical axis is therefore important for waveplate manufacturing and quality insurance. To accurately measure the induced retardation, various methods have been developed, including those based on the mechanical rotation [2-6], polarization modulation [8-11], and scanning interferometry [12-13]. However, all of those methods have their own short comings: the mechanical rotation methods suffer from slow speed and mechanical wear-and-tear, the polarization modulation methods are expensive and complicated, and the

scanning interferometry method cannot simultaneously determine the optical axis of the optical waveplates, in addition to its high cost.

In previous publications, we reported a novel polarization state generator (PSG) [14] and polarization state analyzer (PSA) [15] using four or six binary magneto-optic (MO) rotators. It is a common practice to use a pair of PSG & PSA to fully characterize a waveplate [1], however, such an approach may be excessive, because a PSG/PSA pair not only can measure linear retardation and orientation important to a waveplate, but also other polarization properties, including optical activity and attenuation, which are negligible in optical waveplates. In this paper, we propose and demonstrate a new scheme for waveplate analysis, which is considerably simpler in construction and therefore cost less than a complete PSG/PSA pair. In addition to advantages intrinsic to MO rotators, including no moving parts, compact, fast, superior repeatability and stability, the proposed waveplate analyzer (WPA) can accurately measure the retardation of the waveplate and the orientation of optical axes simultaneously.

2. Principle

The proposed MO-rotator based waveplate analyzer (WPA) with the aperture of 1mm is shown in Fig. 1. Polarizer P_1 is placed at the input of the system and is aligned 22.5° with respect to the fast axis of the $\lambda/4$ waveplate (QWP) to generate a right-hand elliptically polarized light ($S_1=0.5$ $S_2=0.5$ $S_3=0.707$). The waveplate under test (sample) is inserted in the middle slot. Two pairs of MO polarization rotators are placed before and after the sample respectively to rotate light beam's polarization. After passing through the sample, the rotators and a second vertical polarizer (P_2), light finally enters a photodetector (PD) for detecting the optical power changes corresponding to different polarization rotation combinations of the MO rotators. A low-noise transimpedance amplifier and 16-bit A/D converter are used to convert the detected photocurrent to digital signals for further data processing.

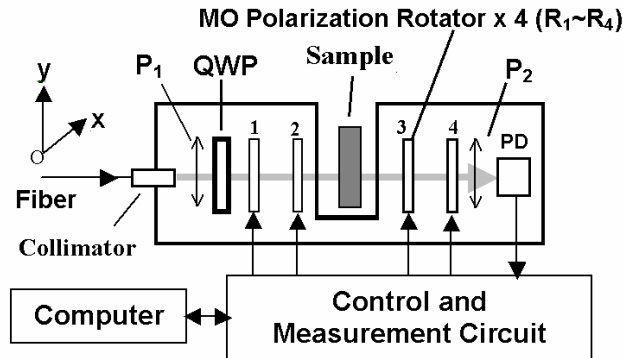


Fig. 1. The proposed waveplate analyzer using 4 MO rotators ($R_1 \sim R_4$): Polarizer P_1 is oriented 22.5° from the vertical axis (y-axis), polarizer P_2 and the fast-axis of $\lambda/4$ waveplate are aligned vertically, and the rotation angles of MO rotators are about $\pm 22.5^\circ$ at their center wavelength.

As in [14] and [15], each MO rotator (2mmx2mm) made from magnetic Garnet crystal can rotate the input state of polarization (SOP) by a precise angle around 22.5° or -22.5° when a positive or negative magnetic field above a saturation field (~ 100 Oe generated by a driving current of 80 mA) is applied respectively. Therefore, when two rotators rotate in the same direction, the net rotation is $+45^\circ$ or -45° . On the other hand, if two rotators rotate in the opposite direction, the net polarization rotation is zero. One may see from Fig. 1 that the power detected by the photodetector will change when the rotation angles of different MO rotators are changed. For different retardance and axis orientation of the waveplate sample under test, the changes in detected power are different for the same rotation combinations of MO rotators. As will be shown next, the retardance and axis orientation of the waveplate

sample can be uniquely determined from the power measurements corresponding to different rotation combinations of MO rotators.

In general, the optical power detected by the photodetector can be written as:

$$I_{\text{out}} = \frac{\kappa I_0}{2} \left\{ 1 + [-\cos 2(\alpha - \theta_{\text{wp}}) \cos 2(\beta + \theta_{\text{wp}}) + \sin 2(\alpha - \theta_{\text{wp}}) \sin 2(\beta + \theta_{\text{wp}}) \cos(\Gamma)] S_1 \right. \\ \left. + [\sin 2(\alpha - \theta_{\text{wp}}) \cos 2(\beta + \theta_{\text{wp}}) + \cos 2(\alpha - \theta_{\text{wp}}) \sin 2(\beta + \theta_{\text{wp}}) \cos(\Gamma)] S_2 \right. \\ \left. + \sin 2(\beta + \theta_{\text{wp}}) \sin \Gamma S_3 \right\} \quad (1)$$

where I_0 is the input optical power entering the analyzer, κ is the attenuation coefficient when taking into account of the insertion loss of all components, $(S_1 S_2 S_3)$ are the normalized Stokes parameters of the light after passing through P_1 and QWP, θ_{wp} is the orientation angle of the fast axis of the waveplate sample with respect to the horizontal, and Γ is the retardance of the sample. The angles α and β are the total polarization rotation angles of the first pair of rotators (before the sample) and the second pair of rotators (after the sample), respectively, and they can be written as

$$\alpha = \sum_{n=1}^2 -(-1)^{b_n} \theta \\ \beta = \sum_{n=3}^4 -(-1)^{b_n} \theta \quad (2)$$

where b_n (0 or 1) is the binary value of the n^{th} rotator (i.e. 0- or 1- state corresponds to negative or positive saturation field applied, respectively), $\theta=22.5^\circ+\Delta\theta$ is the absolute rotation angle of each MO rotator when a magnetic field above saturation field is applied, and $\Delta\theta$ is the deviation angle from 22.5° , caused by temperature and operating wavelength deviations.

Because of the binary nature of the MO rotators, I_{out} has 16 possible values. One can easily find by inspecting Fig. 1 or Eq. (2) that α and β each has three possible values (0, 2θ , -2θ). Therefore, I_{out} in Eq. (1) has $3 \times 3 = 9$ different values for all 16 rotation combinations or logic states, as shown in Table 1. The rests are degenerate.

Table 1: Relationship of a, b and logic states of rotators

I_j	α_j	β_j	Logic States ($R_1R_2R_3R_4$)
I_1	0	2θ	0111, 1011
I_2	0	0	0101, 0110, 1001, 1010
I_3	0	-2θ	0100, 1000
I_4	2θ	2θ	1111
I_5	2θ	0	1101, 1110
I_6	2θ	-2θ	1100
I_7	-2θ	2θ	0011
I_8	-2θ	0	0001, 0010
I_9	-2θ	-2θ	0000

It is clear by inspecting Eqs. (1) and (2) that power I_{out} is a function of the following 7 parameters: $I_0, S_1, S_2, S_3, \theta, \theta_{\text{wp}}$ and Γ . Therefore Eq. (1) for different non-degenerate states can be rewritten as:

$$I_j = f(\alpha_j(\theta), \beta_j(\theta), I_0, S_1, S_2, S_3, \theta_{\text{wp}}, \Gamma), \quad j=1, 2, \dots, 9 \quad (3)$$

where I_j is the output power of the WPA for the j^{th} non-degenerate state (see table 1) and f represents the right hand side of Eq. (1). Assuming the Stokes parameters (S_1, S_2, S_3) generated by P_1 and QWP (Fig. 1) are known, then input power I_0 , rotation angle θ , retardance Γ and axis orientation θ_{wp} of the sample can be calculated by numerically solving Eq. (3). We choose to solve Eq. (3) by numerically searching for the optimized values of $I_0, \theta, \theta_{\text{wp}}$ and Γ to minimize $\sum_j (I_{j,\text{Fit}} - I_{j,\text{Exp}})^2$, where $I_{j,\text{Exp}}$ is the experimentally measured output power of

WPA for the j^{th} non-degenerate state and $I_{j,\text{Fit}}$ is the calculated power using Eq. (3). To ensure high accuracy measurement for waveplates of all possible retardances and orientation angles, we choose to set the SOP of the input light to be around (0.5, 0.5, 0.707) by aligning P_1 and QWP with a relative angle of 22.5° to each other. However, because this input SOP will change slightly as a function of wavelength and temperature due to the wavelength and temperature dependences of the QWP, it is necessary to calibrate the SOP of the input light for different wavelengths and temperatures for high accuracy measurements. Such an SOP calibration can be accomplished by simply measuring the I_{out} for all MO non-degenerate rotation combinations before inserting a waveplate for test. When no sample is inserted, the output power of the WPA for the j^{th} non-degenerate state can be rewritten as

$$I_j = \frac{KI_0}{2} [1 - \cos 2(\alpha_j(\theta) + \beta_j(\theta))S_1 + \sin 2(\alpha_j(\theta) + \beta_j(\theta))S_2] \quad (4)$$

$$= f_j(I_0, \theta, S_1, S_2, S_3)$$

Because the light is totally polarized (ensured by polarizer P_1 in Fig. 1), the following relation holds [16]:

$$S_1^2 + S_2^2 + S_3^2 = 1 \quad (S_3 > 0) \quad (5)$$

Therefore, after measuring the output powers under different non-degenerated states of MO rotators, (S_1, S_2, S_3) can be calculated by solving Eqs. (4) and (5) using the least-square-fitting algorithm.

3. Measurement results

We measured the retardance and the axis orientation of a waveplate sample using the following procedures: (i) The SOP of the input light is determined by measuring the I_{out} under 9 non-degenerate logic states before inserting a waveplate sample [using Eqs. (4) and (5)]. (ii) I_{out} under 9 non-degenerate logic states are measured after the waveplate sample is inserted; and (iii) the least-square-fitting algorithm is used to calculate the parameters in Eq. (3) including the retardance Γ and orientation angle θ_{WP} of the sample by using SOP obtained in step (i). The total measurement time including calculating is less than 0.2 second for one measurement. The typical measured and fitted data are shown in Fig. 2. All measurements are taken at 1550 nm and $23 \pm 2^\circ\text{C}$, and the photodetector outputs have been normalized using the input optical power. The nonlinear least-square-fitting results are shown in table 2. The error factor σ between the measured and fitted data is calculated as

$$\sigma = \sum_j \sqrt{\frac{(I_{j,\text{Exp}} - I_{j,\text{Fit}})^2 / I_0^2}{9}} \quad (6)$$

where $I_{j,\text{Exp}}$ is the experimentally measured output power of WPA for the j^{th} non-degenerate state and $I_{j,\text{Fit}}$ is the calculated output power of WPA for the the j^{th} non-degenerate state using least-square-fitting. The low fitting error σ of 0.0016 shows that Eq. (1) can accurately describe the current WPA system. The measured retardance of 90.4° and 179.64° of the commercial quarter-wave and half-waveplates are consistent with the datasheet from the vendors ($90^\circ \pm 0.7^\circ$, and $180^\circ \pm 0.7^\circ$, respectively). Using the same setup, we also measured the retardance of the air (without any waveplate sample) to be close to zero (as low as 0.057° ,

see Table 2), which indicates the resolution of the measurement. In addition, one hundred measurements with five-second interval are taken to evaluate the repeatability and stability of our WPA system. The standard deviations of the measured retardance are 0.024° and 0.014° for the half-wave and quarter-wave plate, respectively. The corresponding standard deviation of the orientation angles of the optical axes are 0.070° and 0.014° , respectively.

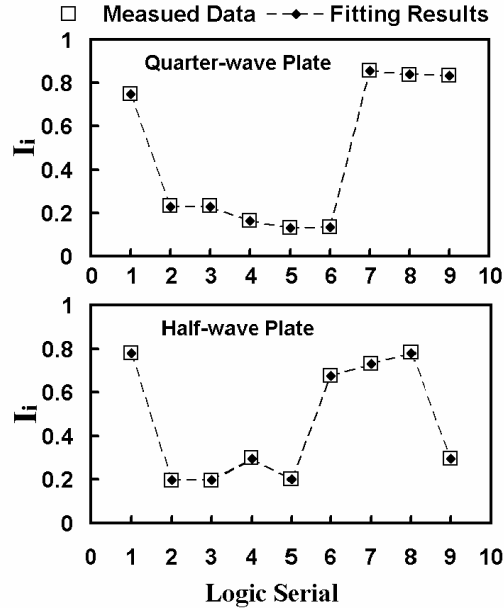


Fig. 2. Typical measurement results with the normalized intensity for the half- and quarter-wave plate. The dash lines are for reference only

Table 2:Least-square-fitting results for different wave plates

	Half-wave Plate	Quarter-wave Plate	Air (no waveplate)
SOP of the input light	$S_1=0.494, S_2=0.514, S_3=0.701$		
Least-square-fitting results			
Retardation of waveplate Γ	179.68	90.41°	0.057°
Orientation angle of waveplate θ_{WP}	-2.24°	89.51°	15.12^*
Rotation angle of rotators θ	21.77°	21.75°	21.74°
Fitting error σ	0.0016	0.0015	0.0008
* The orientation angle of the air is theoretically arbitrary because the air is isotropic. The number given by our measurement system is dependent on the initial input values for the nonlinear least-square-fitting.			

Using a tunable laser, the MO-based WPA can easily acquire the wavelength dependence of both the retardance and orientation angle of a waveplate. The typical measured curves are shown in Fig. 3. The slopes of the retardance are $\sim -0.064^\circ/\text{nm}$, $-0.129^\circ/\text{nm}$ and $-2.701^\circ/\text{nm}$ for a zero-order quartz quarter-wave (WP1), zero-order half-wave plate (WP2) and multi-

order half-wave plate (WP3), respectively. According to the slopes and the chromatic dispersion of quartz crystal, the order of these wave plates can be calculated to be 0, 0, and 10, which are consistent with the data provided by vendors. The standard deviations of orientation angles are 0.12° , 0.045° and 0.23° for WP1~3 in the wavelength range of 1500 nm~1590 nm, respectively.

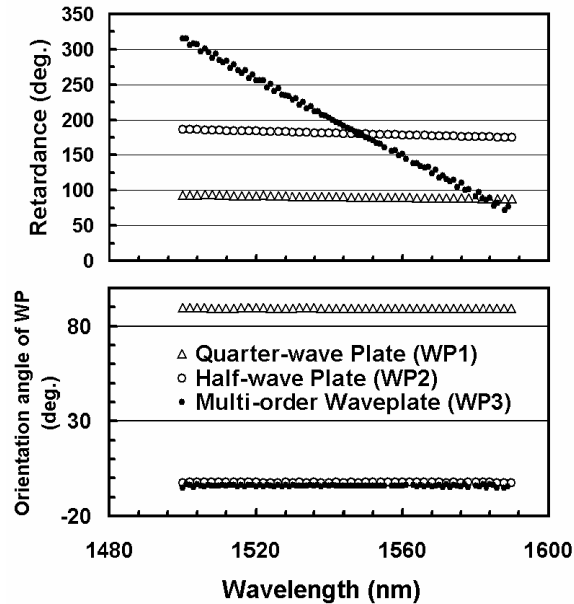


Fig. 3. Typical wavelength dependence curves of the retardance and orientation angle of waveplates measured by our WPA

4. Conclusions

In summary, we demonstrated a novel MO based waveplate analyzer for measuring the retardance, the waveplate order and the orientation angle of a waveplate simultaneously, with high accuracy, repeatability and stability. The device provides an accurate alternative for fast waveplate characterization.